CONEM 2022
CONGRESSO NACIONAL DE ENGENHARIA MECÂNICA
TERESINA - PI

ABCM

XI CONGRESSO NACIONAL DE ENGENHARIA MECÂNICA
DE 07 A 11 DE AGOSTO DE 2022, TERESINA-PI, BRASIL

SHELL AND TUBE HEAT EXCHANGER WITH HELICAL BAFFLES: A PARAMETRIC THERMAL-HYDRAULIC ANALYSIS

Rafael Alberto de Araujo Silva, e-mail rafael.alberto@ufpe.br [1]
Jorge R. Henríquez, jorge.guerrero@ufpe.br[1]
José Ângelo Peixoto da Costa, angelocosta@recife.ifpe.edu.br[2]

[1]Universidade Federal de Pernambuco, Departamento de Engenharia Mecânica, Programa de Pós Graduação em Engenharia Mecânica, UFPE, Recife, PE, Brasil
[2]Instituto Federal de Pernambuco, Engenharia Mecânica, IFPE, Recife, PE, Brasil

Abstract: Heat exchangers are a widely used equipment in both industry and non-industrial applications. The classic example of an industrial application for heat transfer is the shell and tube heat exchanger. This model of heat exchanger varies in size, in tubes profile, quantities, fluid direction and baffle geometries, which can increase thermal efficiency and to reduce pumping costs. The field of study of heat exchangers is not new to science, but when the baffle geometry is changed for a determined application, the performance can vary widely. The present study aims to investigate and compare different heat exchanger's baffle geometry and its effect for overall heat transfer and equipment. The study was conducted through Ansys CFX software with nine different inputs for each geometry, the analysis was conducted by solving the mass, momentum and energy conservation equations through Conjugate Heat Transfer (CHT) analysis. To understand turbulence, the standard k-epsilon model was utilized to simulate turbulent flow. The geometries studied were continuous helical (CH) with the setups of 360º and 1080º; segmented helical (SH) baffles, both for the same sized heat exchanger with a counterflow configuration. The cold fluid inputs were (0.051 kg/s, 0.1kg/s and 0.2kg/s) at 25ºC. The hot fluid inputs were (60ºC, 50ºC and 40ºC) for 0.05kg/s, both analysed fluids were water. The results have shown that for overall equipment performance, the SH configuration has shown the best results for any given hot inlet temperature and cold fluid flow. An interesting finding happens for lower temperature inlet, which the design performs significantly better than CH configurations. For an economic point of view, the higher ratio h/Δp seen for the SH design must be considered as an indicator for the industry. The decreased energy consumption by lower pumping power can represent a more competitive operational cost. On the other hand, when the best thermal performance is to be achieved, the 1080CH baffle configuration has performed better than any other geometry, showing a very relevant finding about continuous baffles for the inputs presented in this work, being an alternative when the highest temperature exchange application is necessary. For most of the inputs, the 360CH shown the worst overall equipment and thermal performance.
Keywords: *Shell-and-tube Heat Exchanger, Helical baffles, Sextant Configuration, Continuous Helical baffles, Circumferential overlap.*

1. INTRODUCTION

According to the first law of thermodynamics, every kind of energy is transferred in a format of work of heat. As it is known, most of daily use equipment require heat transfer to maintain its integrity and to be free of excess heat. Heat exchangers are amazing equipment which can remove excess heat generated by different sources, avoiding overheating and possible component failure. This characteristic allows most of modern electronics to have a high-powered processor, such as a laptop, PC, smartphones and tablets. In the industry, the classic example of a heat exchanger is the shell and tube design. This classic design allows heat transfer through conductive and convective mechanism, without the need of blending. This allows most of fluids to be utilized, but it is mostly used for liquid applications. This design is also extensively studied in experimental and numerical applications, also called Computational Fluid Dynamics (CFD) simulations, Somasekhar et. al (2018). The goal of heat exchangers is to transfer energy in format of temperature, between fluids (water, nanofluids, gases, oil…). The conduction and convection are the heat transfer mechanisms which allows this energy transfer to happen. For the classic format: shell and tube heat exchanger, two fluids with different working temperatures are necessary. The design consists of circular tubes, a shell and baffles. Both cold and hot fluids are pumped to different reservoirs and they are not mixed in the process, the cold fluid has the objective to absorbs the highest amount of heat as possible, and the hot fluid needs to reach the reservoir at the lowest possible temperature. To enhance heat transfer, some mechanisms can be applied. Some authors suggests that a larger equipment can be utilized, but this application can be limited due to its size and weight, Bichkar et al. (2018).

To be efficient as possible, a hight heat transfer coefficient is required to the heat exchanger. A higher mass flow at cold side is also another parameter that must be controlled to increase heat transfer, but at the same time, the pressure drop must be small for overall efficiency. To achieve a higher efficiency, it is well known by the literature that counter flow configuration performs better compared to parallel. The baffles also, play a main role in this part, as they are responsible for most of the turbulence due to its format. The turbulence is caused to enhance heat transfer between fluids, but it can also increase pumping losses, decreasing the overall efficiency of the equipment. To achieve a higher heat transfer with the lowest possible pressure drop, baffles with different shapes were proposed and extensively studied in shell and tube heat exchangers, Bichkar et al. (2018).

Following the studies of options to increase heat transfer without adding significant pressure drop, the idea of segmented baffles came as a realistic option. Segmented baffles were found to create most of the pressure drop if compared to "flower" and helical configurations. The drop is mainly caused by velocity jets and fluid recirculation, being crucial due to heat exchanger operating costs. On the other hand, continuous helical configurations can have a relative easier construction and demonstrate a higher performance for some configurations. In industrial applications, cooling high powered engines is very challenging. Even if it is possible to introduce very large heat exchangers, it can quickly become costly. Trying to achieve a higher efficiency using the same equipment, scientists have tried to improve the design, changed construction materials, working temperatures and other configurations to optimize heat exchangers, Bahiraei et al. (2015).

Through the recent years, CFD is becoming more popular due to the high cost of experimental studies and the decreasing price of standard personal computers, which usually carry very powerful processors. This tool became commonly used to study fluid flow, heat transfer and chemical reactions associated with the system. It can predict how fluid will behave in distinctive environments and mechanical applications. Using the Navier-Stokes equation, iteratively the Computer Aided Engineering (CAE) software can solve equations for conservation of momentum, mass and energy for the analysed system.

Although studies involving heat exchangers with different geometric baffle schemes are found in the literature by Bahiraei et al. (2015), Ghanbari et al. (2015), Lima (2020), the question of what kind of heat exchanger baffle scheme can achieve a better performance still remains. In this study, three helical baffle heat exchangers: 360-degree continuous helical (360CH), 1080-degree continuous helical (1080CH) and segmented helical (SH) designs were compared (40º helix angle with overlap) were compared, and water was chosen as the working fluid for both hot and cold domains. All designs are developed for the same heat exchanger layout, with different baffle shapes.

2. MODELLING DETAILS

2.1. The Geometry

The Computed Aided Design (CAD) software, commercial Solidworks 2019 was the choice for the design created and shown in Figure 1. The model was first created and then exported to ANSYS DesignModeler, which later the geometry was submitted to a Conjugate Heat Transfer (CHT) Analysis, allowing simulation for different domains: solid and fluid. This analysis occurs by the exchange of heat energy happening in the interface between these surfaces. The geometry is a shell and tube heat exchanger. For the hot fluid domain, there are 7 tubes for hot fluid flow converging into a conical structure for the hot outlet. For the cold fluid domain, the flow is forced through the baffles, creating a slalom move profile.

Figure 1 shows the experimental heat exchanger in CAD, being the model used to compare experimental and numerical results, validating the chosen methodology.

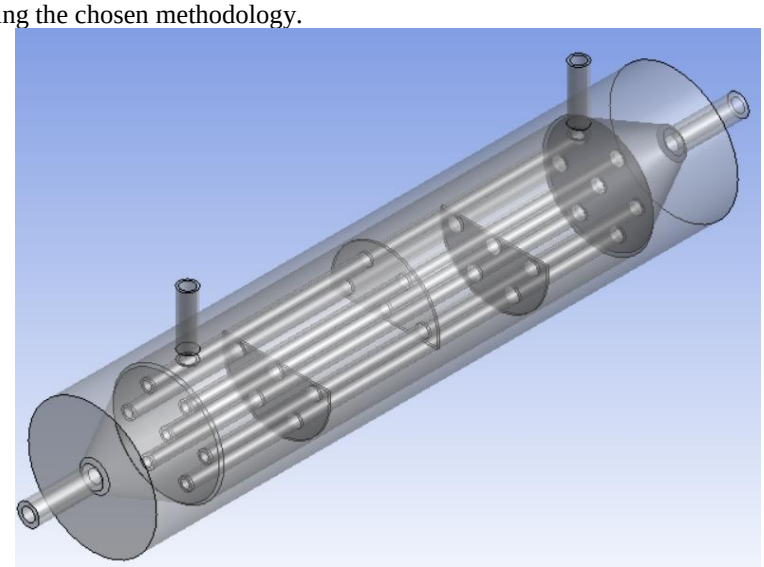

Figure 1. **Trimetric view of the original heat exchanger**

Although, the main purpose of this paper is to study geometry differences influence in the behaviour of heat transport with different water, for this reason, the modified geometries are shown in Figure 2, which also shows the section view of each different baffle scheme.

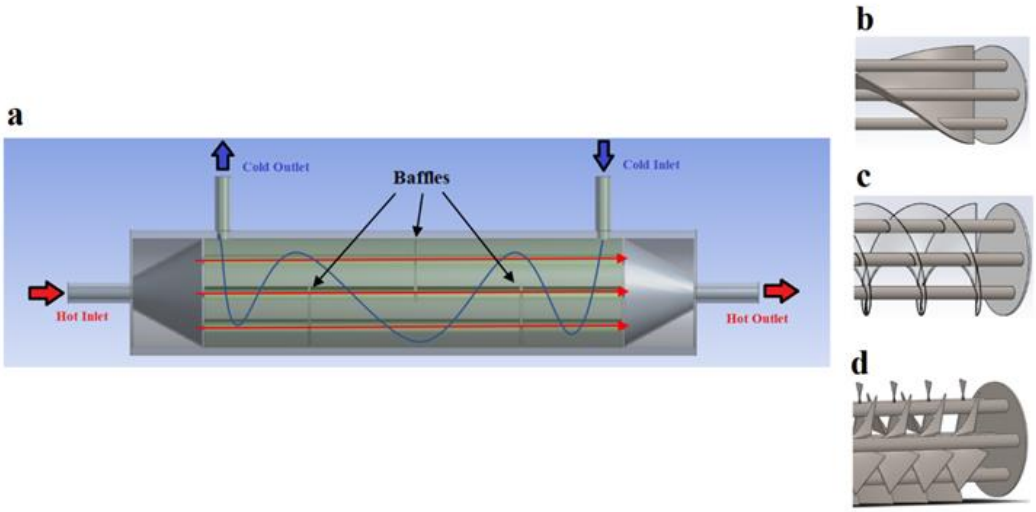

Figure 2. **Geometric model of the heat exchanger and three baffle structures. (a) Geometric model and flow directions, (b) 360CH baffle detailed view, (c) 1080CH baffle detailed view, (d) SH baffle detailed view.**

Its geometric parameters can be seen in Table 1, these particular characteristics allow fluid flow behaviour to change. The continuous helical (CH) geometries were created in two different shapes, varying the baffle angle rotating on its own axis by 360^0 and 1080^0. The segmented helical (SH) represents a helical spiral is formed by sextant geometry with a helix angle of 40^0.

Table 1. **Geometric parameters of helical baffles**

ITEM	360 CH	1080CH	SH
Shape	Continuous	Continuous	Segmented Sextant
Helix Angle (^{0})	43.36	70.56	40
Helix Pitch (mm)	173	57.66	69.01
Overlapped space (mm)	-	-	2.21
Baffle number	1	1	55
Baffle thickness (mm)	0.5	0.5	0.5
Axial overlapped ratio (%)	-	-	8.5

2.2 Governing Equations and Boundary Conditions

The approach chosen to model the shell and tube heat exchanger is the Conjugate heat transfer (CHT) analysis. This method involves solving the mass, momentum and energy conservation equations. For the solid domain, the conservation of energy equation can account for the transport of heat, due to solid motion, conduction and volumetric heat sources. For the turbulence model, the widely used is the k-epsilon turbulence model and its variants. The method is utilized for turbulence flow and it is part of the Reynolds-averaged Navier-Stokes (RANS) family (which describes all turbulence effects), modifying the original unsteady Navier-Stokes equations into a statistical model representing mean flow quantities only, found at Simscale (2021). The following governing equations are for the continuity, momentum and conservation of energy in the computational domain for an incompressible and Newtonian fluid.

- Continuity equation

$$\nabla\left(\rho_{eff}\bar{V}\right) = 0 \tag{1}$$

- Momentum equations

$$\nabla\left(\rho_{eff}\overline{V}\overline{V}\right) = -\nabla\overline{P} + \mu_{eff}\nabla^2\bar{V} - \rho_{eff}\nabla\left(\overline{v'v'}\right) \tag{2}$$

- Conservation energy

$$\nabla\left(\rho_{eff}C_{p,eff}\bar{V}\bar{T}\right) = \nabla\left(\left(k_{eff} + k_t\right)\nabla\bar{T}\right) \tag{3}$$

For these equations, components $\overline{V}, \overline{T}$ and $\overline{\mathrm{P}}$ represents the time averaged flow variables, while v' is the velocity fluctuations. The turbulent term of shear stress is $\rho_{eff}\nabla(\overline{v'v'})$, k_{eff} is the effective molecular conductivity and k_t stands for the turbulent thermal conductivity. The turbulent Regime is determined by Reynolds' number, for this flow level of agitation, the standard k- ϵ model is represented by the following equations.

- Turbulent kinetic energy

$$\nabla(\rho_{eff}kV) = \nabla\left[\left(\frac{\mu_t}{\sigma_k}\right)\nabla(k)\right] + G_k - \rho_{eff}\varepsilon \quad (4)$$

- Turbulent energy dissipation

$$\nabla(\rho_{eff}\varepsilon V) = \nabla\left[\frac{\mu_t}{\sigma_\varepsilon}\nabla\varepsilon\right] + \frac{\varepsilon}{k}(C_{1\varepsilon}G_k - C_{2\varepsilon}\rho_{eff}\varepsilon) \quad (5)$$

Where, $\mu_{eff} = \mu + \mu_t$, $\mu_t = \frac{\rho_{eff}C_\mu k^2}{\varepsilon}$, $G_k = \mu_t(\nabla V + (\nabla V)^T)$, and μ_{eff} and μ_t respectively represents the effective viscosity and viscosity coefficient for turbulent regime. The process of discretization, which is the transfer of function, models, variables and continuous equations into suitable numerical evaluation was made by Ansys CFX. The CFX solver was the chosen software to be implemented, it uses finite volume method. The Turbulence was solved by First Order method. The number of iterations were set to a maximum of 2000 or the convergence criterion was reached. The convergence only happened if the established limit to residuals by RMS (Root mean square) was reached. The specified value is that the normalized absolute residuals are less than 10^{-4}, which is sufficient for this problem. The pure water is always both fluids: cold and hot. The medium is steady-flow with turbulence, and the fluids are considered incompressible.

Fluid properties are according to Table 2. The hot domain stands for the hot inlet, outlet and the interface. The heat transfer model is thermal energy. The inlet is kept at static temperature (40ºC, 50ºC and 60ºC) and flow regime is set to be subsonic and the mass flow rate number is 0.051 kg/s. Turbulence model is k-Epsilon with wall function scalable. The entire domain is non-buoyant, and the motion is stationary. Inlet is kept at constant temperature (25ºC) and the fluid flow is set to be subsonic (0.01 kg/s, 0.025 kg/s, 0.05 kg/s). The pressure outlet boundary conditions are applied on outlets of shell side and tube side, the pressure values of outlets are set to 0 Pa (gauge pressure). The solid domain is composed by Steel contained in ANSYS CFX material library. Heat transfer is conservative interface flux, the momentum boundary for all solid surfaces is non-slip and the roughness is negligible, being smooth wall.

Table 2. **Thermophysical properties of water**

Wt %	k (W/mK)	ρ (Kg/m³)	μ(Kg/ms)	Cp (J/kg.k)	T (°C)	Pr
Water	0.62	937.5	0.000891	4120.0	25	5.92

2.3. The Mesh

2.3.1 Grid Generation, independence and analysis

ANSYS Meshing software was responsible for mesh generation, the 3D grid was created for later mathematical modelling. Three different meshes were first generated to meet the criterium defined at the last section. The best solution is always the most approximate to experimental results and the one which represents less computational costs, that is the reason for the mesh comparison. The meshes are as follows: extra refined, refined and simplified, being seen at Table 3.

Table 3. **Mesh parameters**

ITEM	Segmented Sextant		
Grid	Extra refined grid	Refined Grid	Simplified Grid
Elements	1465052	758858	280945
Nodes	21230003	10696546	421325
Element type	Tetrahedron	Tetrahedron	Tetrahedron
Inflation	Yes	Yes	Yes
Element Order	Quadratic	Quadratic	Quadratic
Sizing	Face Sizing / Element Sizing/Patch Conforming	Face Sizing / Element Sizing/Patch Conforming	Face Sizing / Element Sizing/Patch Conforming

For the convergence, the minimum requirements were: 1- Residual value u, v, w, k and ε met the value to be less than 10^{-4} and convergence was achieved; 2 – Outlet hot fluid temperature did not exceed 2% deviation to experimental result. The extra-refined mesh took 08:59:23 to complete the simulation with 1229 iterations to achieve convergence. The refined took 05:16:32 for 1396 iterations, the simplified took 02:54:35 at 1448 iterations. A lateral cut from the mesh can be seen in Figure 4.

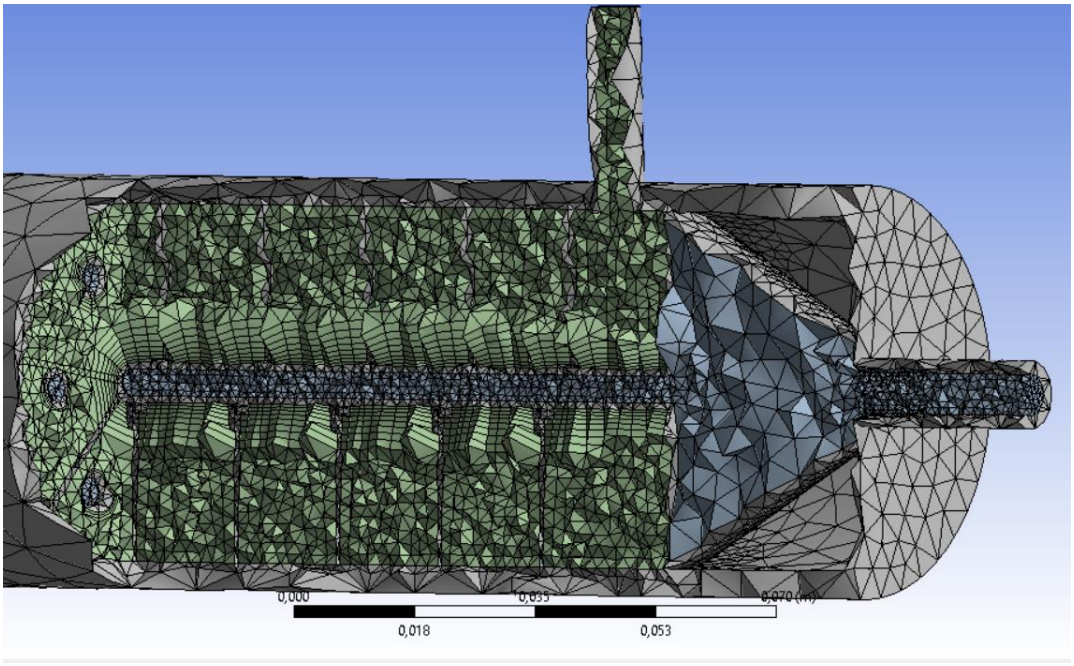

Figure 4. **Refined mesh cut**

The outlet hot fluid temperature was 55.80ºC, 56.04ºC and 55.98ºC for the simplified, refined and extra-refined grid respectively. For the requirements 1 and 2, all three meshes complied. To validate turbulence model, y^+ and wall shear stress were analysed. The standard wall function, which was utilized for the turbulence model k-Epsilon needs a $\boldsymbol{y}^+$ value varying between 30 to 300 [26], which happened mostly in the geometry. For the simplified mesh, $\tau_s = 0.282098$ [Pa], for the refined mesh, $\tau_s = 0.357787$ [Pa], and for the extra-refined mesh, $\tau_s = 0.342431$ [Pa]. The simplified mesh has a 21% divergent result compared to the refined and a 17.61% difference from the extra-refined. For the refined mesh, the percentage difference with the extra-refined was 4.48%.

2.3.2 Data reduction and model validation

The major equations used in data reduction can be seen as follows. The heat transfer rate of the shell side can be calculated based on Equation (6). Where $\dot{m}$ denotes the mass flow rate in both conditions (shell and tubes). The shell-side heat transfer coefficient is calculated based on Equations (7) to (11). The A_o is the heat exchanger area based on the outer diameter of the tubes multiplied by its number, in this case, 7.

$$Q_{shell} = \dot{m}_{cold} C_{p,cold} \left(T_{cold,inlet} - T_{cold,outlet}\right) \tag{6}$$

The logarithmic mean temperature of the shell ΔT_{lm} for counter-flow pattern can be determined by Equation (9), the correction factor for the logarithmic mean temperature difference is 1.

$$h_{shell} = \frac{Q_{shell}}{A_o \, \Delta T_{lm}} \tag{7}$$

$$A_o = n\pi d_0 l \tag{8}$$

$$\Delta T_{lm} = \frac{\Delta T_{max} - \Delta T_{min}}{\ln\left(\frac{\Delta t_{max}}{\Delta T_{min}}\right)} \tag{9}$$

$$\Delta T_{max} = T_{shell,in} - T_{wall} \tag{10}$$

$$\Delta T_{min} = T_{shell,out} - T_{wall} \tag{11}$$

Even though as the 360CH, 1080CH and SH configuration were all simulated in the same conditions and with high accuracy convergence history (1e-04), heat flux is not equal on the shell-side and on the tube-side, leading to a possible subtle deviation from the CFX solver. As the fluid's outlet temperature is one of the most important parameters of this study, heat transfer rate considered is from the tube-side. Reynolds number was calculated by a method proposed by Alperen et. al (2019) , for helical baffles. The equivalent Diameter (D_e) for the triangular tube alignment, Reynolds number, cross sectional area A_s and baffle spacing e are shown in the following equations:

$$D_e = \frac{4\left(P_t{}^2 - \frac{\pi d_0{}^2}{4}\right)}{\pi d_0} \tag{12}$$

$$R_{e,shell} = \frac{D_e \dot{m}_{hot}}{\mu A_s} \tag{13}$$

$$A_{ss} = 0.639(P_t - d_{outlet})e\sqrt{\frac{CL}{CTP}\frac{A}{d_0 L}} \tag{14}$$

$$A_{scnc} = 0.5e\left[D_{shell} - D_{otl} + \frac{D_{olt} - d_{outlet}}{P_t}(P_t - d_{outlet})\right] \tag{15}$$

Where P_t is the tube pitch, D_e is the shell diameter, A_s is the cross-sectional area of the shell, according to the baffle, A_{ss} stands for the segmental baffles and A_{scnc} for the continuous and noncontinuous and e is the baffle spacing. The Reynolds number, cross sectional area A_s and baffle spacing e are shown. The following data will be described in different cases according Table 4.

Table 4. **Parametric Data Inputs**

	Cold fluid temperature (ºC)	Cold fluid flow rate (kg/s)	Hot fluid temperature (ºC)	Hot fluid flow rate (kg/s)
Input 1	25	0.051	60	0.5
Input 2	25	0.01	60	0.5
Input 3	25	0.2	60	0.5
Input 4	25	0.051	50	0.5
Input 5	25	0.01	50	0.5
Input 6	25	0.02	50	0.5
Input 7	25	0.051	40	0.5
Input 8	25	0.01	40	0.5
Input 9	25	0.02	40	0.5

Table 5 shows the comparison between models of the heat exchanger. The current algorithm used in this paper has shown even a closer result to the experimental work conducted by Lima (2020). Although the difference between both CFD models were small, the mesh developed in this current work was more refined (inflation, smaller element size played a crucial rule in this higher number of elements).

Table 5. **Methodology Proof**

	Experimental Analysis [Simscale (2021)]		CFD Analysis [Lima et. al (2020)]		STHE (CFD)		Difference [%]	
	Inlet	Outlet	Inlet	Outlet	Inlet	Outlet	Exp.	CFD
Cold fluid temperature [ºC]	28.20	32.09	28.20	31.13	28.20	31.53	1.75	1.28
Hot fluid temperature [ºC]	58.46	55.07	58.46	56.04	58.46	55.35	0.51	1.23

3. RESULTS

3.1. Shell-side pressure drop

Figure 5 depicts the effect of fluid flow over pressure drop. The different baffles played a major role for lowering pressure drop at higher fluid flow. At a higher cold fluid flow, pressure drop is more significant, as expected due to energy loss caused mostly by friction and turbulence. The Reynolds shows both laminar and turbulent regime, varying between

422 to 6840. The figure suggests that the Segmented Helical (SH) baffle configuration has shown the lowest pressure drop in any fluid flow scenario. For the lower flow scenario, the pressure drop change is much smaller but also considerable. For 0.1m³/s and 0.2m³/s, the change in the regime from laminar to turbulent can explain the highest pressure drop. The SH has a Reynolds number of 1427 for the 0.051kg/s flow, 2798 for the 0.1kg/s and 5596 for the highest flow (0.2kg/s).

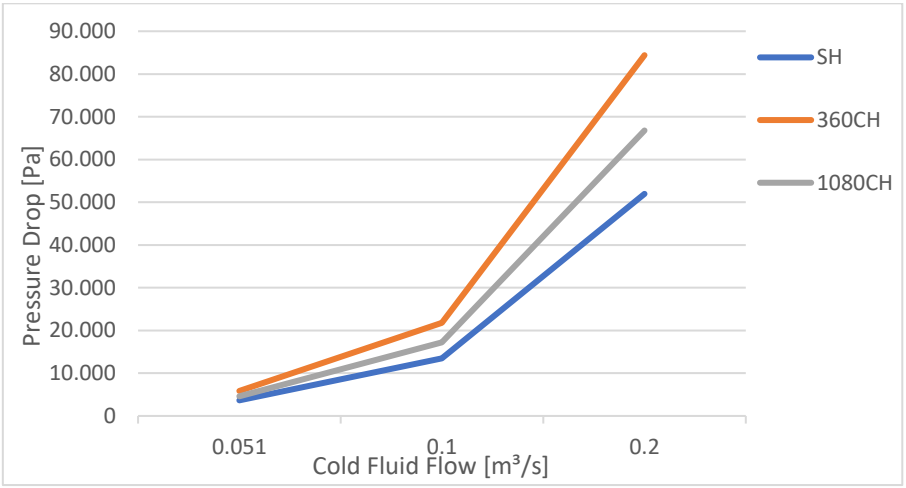

Figure 5. **Shell-side head loss effect**

Even though the 1080 CH configuration presented a lower pressure drop compared to the 360 CH, for this design, the Reynolds number varies from 422, 828 and 1657 respectively for the 0.051, 0.1 and 0.2 kg/s flow. The 360CH has 1250, 2452, 4904 Reynolds number respectively for the same flow from the 1080CH scenario. The 360CH result was somewhat of surprising due to the much lower baffle complexity design compared to the other two. The simplicity was presumed to achieve a lower amount of eddy motion and a significant reduction in pressure drop, but actually the opposite occurred. In Figure 6, the velocity vector contours are evidencing where higher energy losses happens. From the figure, it can be seen that the highest energy loss occurs mostly at cold inlet, when fluid direction is still being defined as it flows through the baffles. For the 360CH, the absence of baffles makes the flow have a concentrated velocity at some points, showing a probable poor flow distribution. From the inlet, higher velocity vectors are seen next to the lower part of the shell, in the middle the velocity is low, leading to what was suggested as poor flow distribution. As flow passes through the heat exchanger, flow distribution improves. For the 1080CH, the lowest Reynolds number is described be the lower velocity flow caused by a good flow distribution over the baffles, this leads to a laminar flow. For the SH configuration, velocity contour is more distributed than the other configurations, probably due to the high number of baffles, increasing fluid collision. Through the shell, flow has a higher velocity at the corners, but has most proportional velocity vectors distribution.

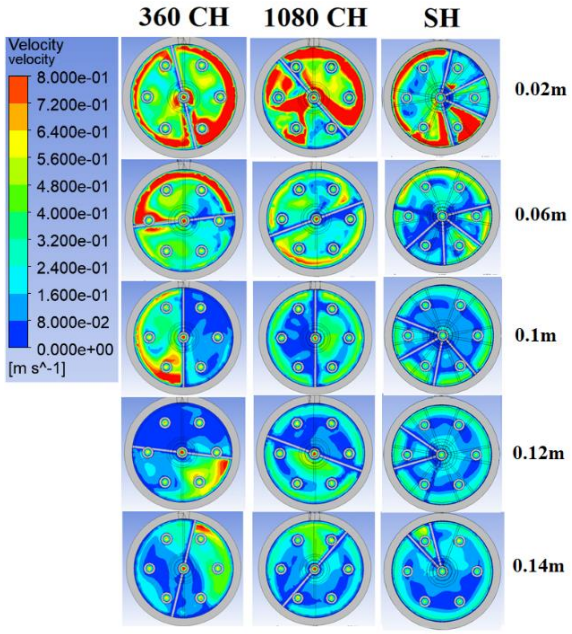

Fig. 6 **Shell side velocity contours comparison in a cross-section view**

3.2 Heat transfer rate

In Figure 7, all 9 different inputs are compared to its respective baffle design. From the evidence, the highest heat transfer rate occurs at higher inlet temperatures, allowing more heat to be transferred from hot tubes to the cold fluid. This energy transfer is enhanced when cold fluid is augmented, and the highest amount can be seen for Input 3, which represents the 0.2m³/s cold volume flow. From the Inputs 1-3 it is also clear that the best-case scenario for heat transfer rate is the 1080CH configuration, allowing more heat to be transferred than at higher temperature inlets. The situation changes when inlet temperature drops to 50ºC, allowing the SH geometry to performs better than the others, showing a significant advantage for the SH at lower inlet temperatures. The performance at highest cold fluid flow is superior for the 1080CH configuration for all different scenarios. The 360CH has shown a significant advantage compares to the SH for the higher temperature inlet, but for all other scenarios, its performance decreases and it turns to be the less advantage geometry.

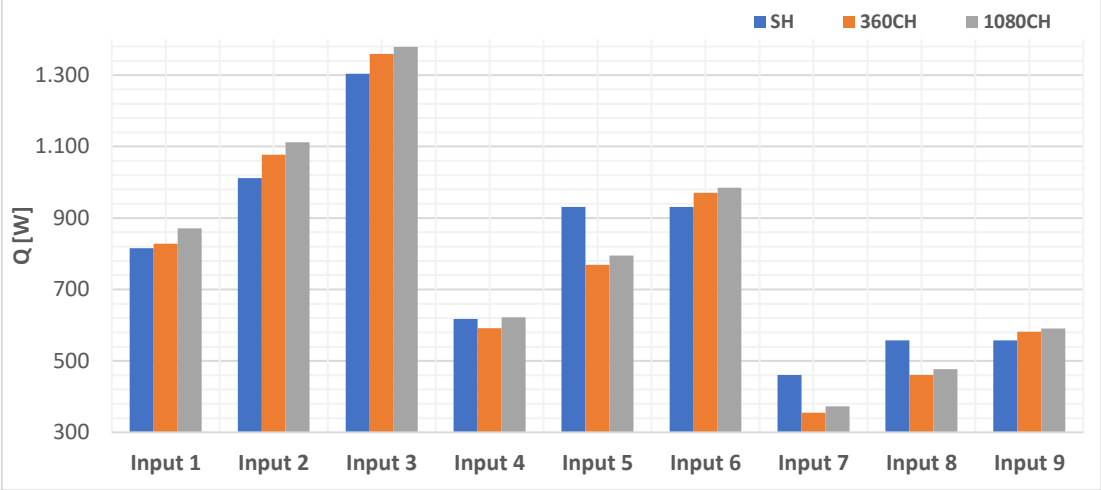

Figure 7. **Heat transfer rate comparison**

3.3 Temperature distribution

The outlet temperature difference can be seen more clearly in Figure 8, which compares each outlet for inputs and heat exchanger design. From this comparison, the advantage for the 1080CH is clear for almost all different temperature inputs, although the advantage seen for the heat transfer rate is confirmed for the SH configuration for lower inlet temperature and cold fluid flow.

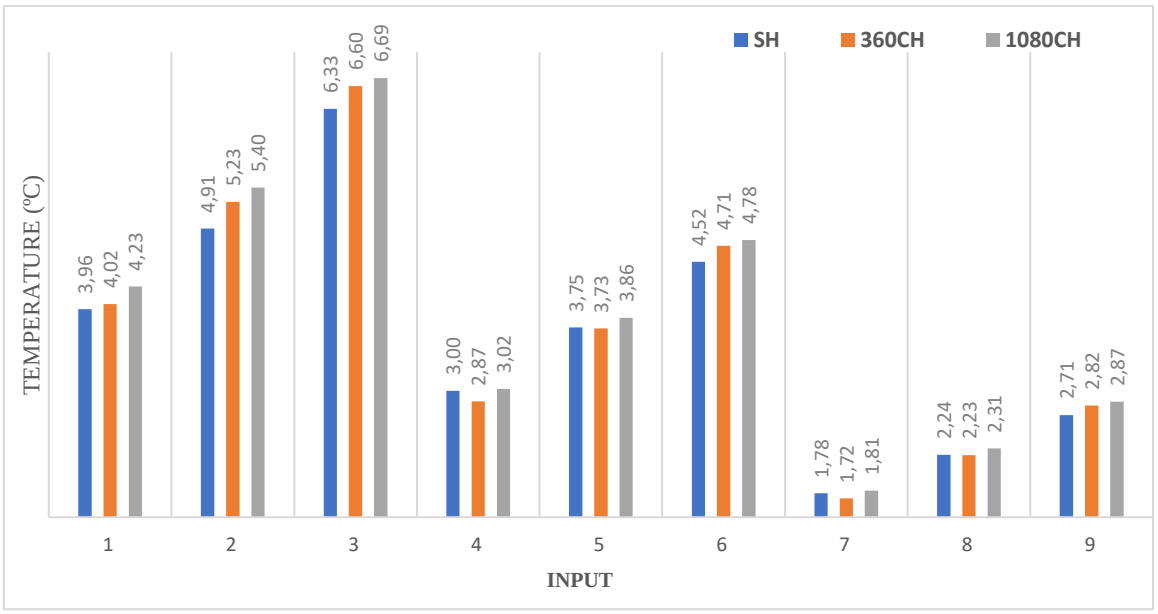

Figure 8. **Outlet temperature comparison**

3.4 Heat transfer rate per pressure drop

From Figure 9, it can be understood that heat exchangers with the lowest helix angles (40º helix angle) have the highest heat transfer coefficient per unit pressure drop for higher temperatures. The difference created by the SH configuration is

significant for all different inputs. The losses from the pressure drop represents a very significant role for the heat exchanger problem. Mostly of the outlet temperature differences obtained by the 360CH and 1080CH were widely surpassed when a thermo-hydraulic analysis is made and understood. As the SH represented the best scenario for all inputs, the 1080CH followed as the second option from this point of view and the worst performance was obtained by the 360CH. An interesting result can be seen for the higher volume flow (i.e. inputs 3, 6 and 9), the significant for each heat exchanger starts to become less significant, and it leads to believe if cold fluid flow rate was increased it would become insignificant, leading us to choose for the better temperature outlet instead of an overall performance evaluation.

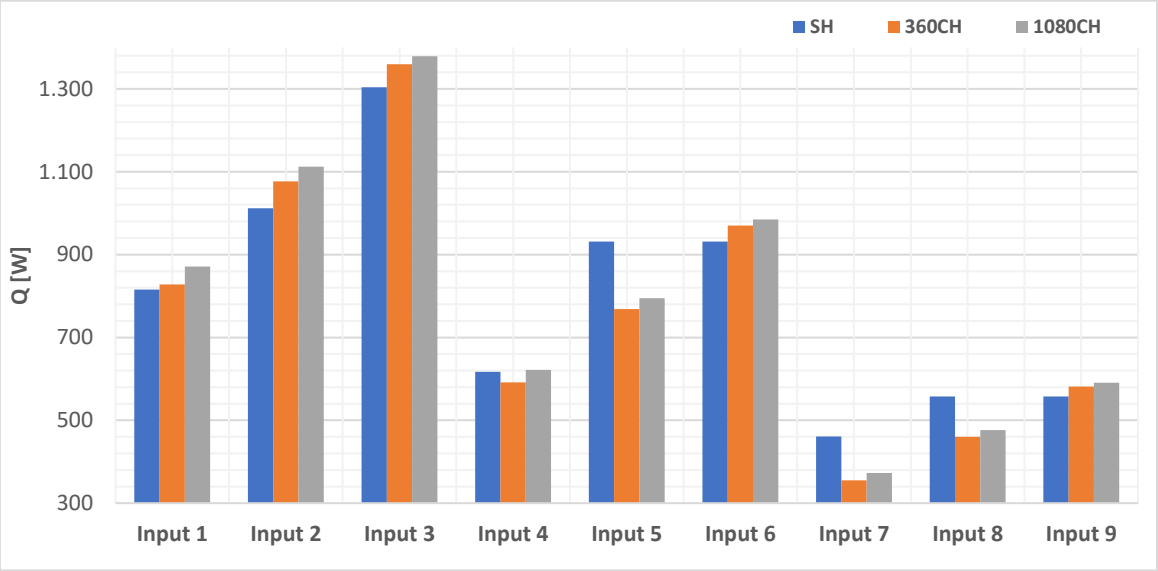

Figure 9. **Heat transfer rate per unit pressure drop versus volume flow rate**

4. CONCLUSION

In this work, shell and tube heat exchangers with different helix baffles were simulated though ANSYS CFX software for heat transfer and flow characteristics in a parametric analysis. A comparison of geometry complexity, baffle characteristics, heat transfer, fluid flow and performance were made to investigate the outcome of nine simulation models. Three different geometries were created in Solidworks CAD software, each one with a different baffle profile: 360º Continuous Helical (CH), 1080ºCH and Segmented Helical. Based on the results of this study, it can be concluded that baffle geometry can significantly contribute to increase of heat transfer and pressure drop. The major findings are summarized as follows: 1 - The SH heat exchanger configuration has shown the least pressure drop even at higher volume flows. The 1080CH comes after and for the last the 360CH. The shell side pressure drop is significantly reduced when baffle helix angle is also small. The SH configuration has shown the smallest helix angle, the 360CH the second smaller and the last the 1080CH. 2 - In a perspective of heat transfer rate, it can be concluded that in general, the best-case scenario is achieved at 1080CH at the highest fluid flow (0.2m³/s). The SH design starts to have a significant advantage for heat transfer rate when inlet temperature drops to 50º and 40ºC. 3 - 1080CH shows the highest temperature outlet for the cold fluid and consequently, the highest temperature difference from cold to hot fluid. 4 - The ratio between Q/Δp have shown that for the 60ºC, 50ºC and 40ºC degree input, the SH shows the best ratio. Lower helix angle from the SH helps to lower friction between wall and fluid. The 1080CH shows a competitive performance compared to the SH geometry and sometimes it is superior, on the other hand the SH surpasses any design when fluid flow losses are accounted, being very important to achieve a higher overall performance. Although the SH has shown an advantage for the Q/Δp ratio, if the main goal is to achieve a higher thermal exchange, the best choice is the 1080CH. There is no significant advantage found in this paper for the 360CH. It is suggested that in further studies, a variation in the baffle angle geometry for the SH and the CH should be made to understand the effects in both heat transfer and energy losses due to friction.

5. ACKNOWLEDGEMENTS

This study was financed in part by the Coordination for the Improvement of Higher Education Personnel (CAPES in Portuguese) - Brazil - Finance Code 001. The second author thank the CNPq (National Council for Scientific and Technological Development -Brazil) for the scholarship of Productivity (Proc.315265/2020-5).

6. REFERENCES

Somasekhar, K., Malleswara Rao, K. N. D., Sankararao, V., Mohammed, R., Veerendra, M., & Venkateswararao, T. (2018). *A CFD Investigation of Heat Transfer Enhancement of Shell and Tube Heat Exchanger Using Al2O3 -Water Nanofluid. Materials Today: Proceedings, 5(1), 1057–1062.*

Bichkar, P., Dandgaval, O., Dalvi, P., Godase, R., & Dey, T. (2018). *Study of Shell and Tube Heat Exchanger with the Effect of Types of Baffles. Procedia Manufacturing, 20, 195–200.*

Stehlík, P., Wadekar, V.V., (2002). *Different Strategies to Improve Industrial Heat Exchange, Heat Transfer Engineering, 23(6), 36-48, DOI: 10.1080/01457630290098673*

Bahiraei, M., Hangi, M., & Saeedan, M. (2015). *A novel application for energy efficiency improvement using nanofluid in shell and tube heat exchanger equipped with helical baffles. Energy, 93, 2229–2240.*

Lei, Y.-G., He, Y.-L., Chu, P., & Li, R. (2008). *Design and optimization of heat exchangers with helical baffles. Chemical Engineering Science, 63(17), 4386–4395.*

Dong, C., Chen, Y.-P., & Wu, J.-F. (2015). *Flow and heat transfer performances of helical baffle heat exchangers with different baffle configurations. Applied Thermal Engineering, 80, 328–338.*

Simscale Thermal Simulations 2021, accessed 29th May 2021, <https://www.simscale.com/docs/simulation-setup/global-settings/k-epsilon/>

Lima, C. C. X. S (2020) *Estudo teórico e experimental da transferência de calor utilizando nanofluidos em trocadores de calor, M.Sc. Thesis, Universidade Federal de Pernambuco, Recife, Pernambuco, Brasil, 2020.*

Alperen, M. A., Kayabaşi, E., & Kurt, H. (2019). *Detailed comparison of the methods used in the heat transfer coefficient and pressure loss calculation of shell side of shell and tube heat exchangers with the experimental results. Energy Sources, Part A: Recovery, Utilization, and Environmental Effects, 1–20.*

U. Ur-Rehman, *Heat transfer optimization of shell–and–tube heat exchanger through CFD studies, M.Sc. Thesis, Chalmers University of Technology, Göteborg, Sweden, 2011.*

7. DECLARATION OF COMPETING INTEREST

The authors declare that they are the only ones responsible for this paper content.